Current Research and Innovations Journal

Research Article

DESIGNING EFFICIENT POWER TOWERS: INSIGHTS FROM NUMERICAL MODELING TECHNIQUES

Tenzin Lhamo Wangchuk

College of Engineering, Tibet University, Lhasa, 850000, Tibet, China

DOI: 10.5281/zenodo.14678000

Abstract

This paper embodies the fusion of theory and practice, as the authors harmoniously blend theoretical insights gleaned from professional coursework with the experiential wisdom accumulated through their work endeavors. The outcome of this synergy manifests in the design and production of a model, seamlessly bridging the realms of practical engineering and theoretical knowledge. The entire process of modeling unfolds as a holistic integration of fundamental mechanical and structural theory, complemented by practical workplace expertise. This synthesis not only fosters the cultivation of hands-on practical skills but also constructs a robust linkage between the spheres of practice and theory. It becomes evident that the quality of model production intricately hinges on the author's practical acumen.

Consequently, this endeavor imparts an unparalleled influence on the authors' cognitive processes and innovation capacity, ushering in a culture of active learning, practical engagement, and comprehensive skill enhancement.

Keywords: Theory and Practice Integration, Model Design, Practical Skills, Engineering Education Active Learning

1. Introduction

In this paper, the authors unite theory and practice, apply theoretical knowledge learned in the main courses of the profession and experience accumulated in the workplace to the design and production of the model, and build a link between real engineering and theoretical knowledge. In the whole stage of model design and production, not only the basic theoretical knowledge of mechanics and structure is applied, but also the practical experience of work and production is applied, which integrates the cultivation of hands-on practical skills and builds a bridge between practice and theory, while the quality of model production is closely related to practical hands-on ability. In turn, it has an unparalleled effect on the author's thinking and innovation, active learning, practical hands-on and comprehensive skill enhancement.

Power pylons are one of the important structural forms of high-rise building structures. How to design and fabricate power pylons and simulate the actual load condition for loading test as required becomes the key and difficult content. In this paper, we will introduce the ideas, structural selection and design, component fabrication and ANSYS numerical analysis.

2. Introduction to the Idea

2.1. Overview of Ideas

Design and make a model of a power tower, the bottom of the model using screws firmly placed in the size of 400mm×400mm×15mm (length×width×thickness) of the board, the size of the bottom of the model made strictly

| ISSN: 3065-0712 Page | 1

<u>Current Research and Innovations</u> <u>Journal</u>

Research Article

controlled in the center of the board 250mm×250mm square range, as shown in Figure 1 a), and the center of the board for the O point [1].

The model is equipped with 2 "low hanging points" and 1 "high hanging point" for subsequent loading to hang the wire, and the "high hanging point" is also used as a "horizontal The "high hanging point" is also used as a "horizontal loading point". The farthest outreach point is called the low hanging point, and the height between the lower base plate surface is limited to $1000_{\sim}1100$ (mm), and the projection formed on the lower base plate surface is in the circular shadow of the upper and lower sectors shown in Figure 1 a); the high hanging point is limited to $1200_{\sim}1400$ (mm), and the height between the lower base plate surface is limited to $1200_{\sim}1400$ (mm), and the projection formed on the lower board surface is not far from the center O Projection, not more than 350mm from the center O point, and the model made by the high point is called high hanging point. The vertical position of the low and high hanging points of the model is shown in Figure 1b) [2].

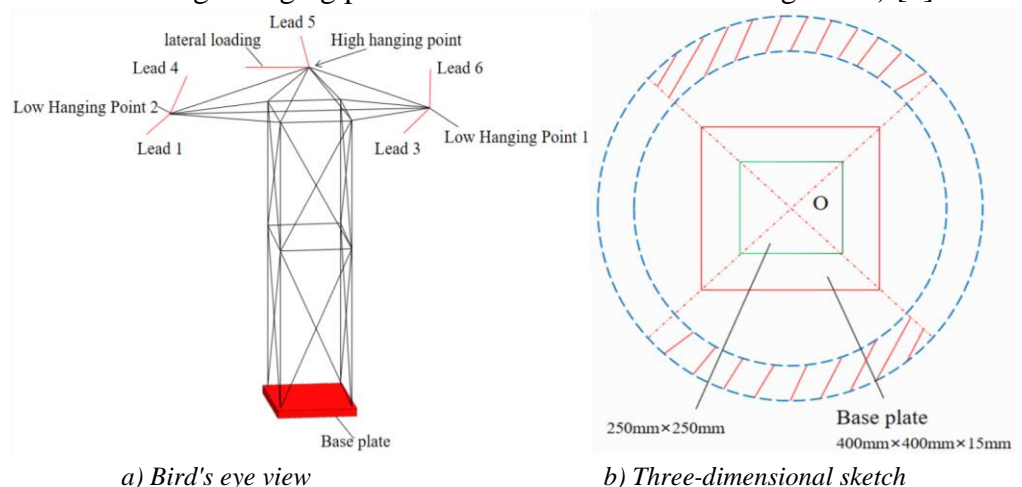


Figure 1: Geometric range conditions of power tower model (mm).

2.2. Material Properties

The materials used for the experiments were bamboo veneer paper and bamboo strips, whose bamboo specifications and material properties are referred to Table 1 and 2 below.

Table 1: Bamboo material specifications.

Type	Specification (length×width×thickness mm)	
Bamboo Veneer 1250×430×0.2 (single layer) 1250×430×0.35 (double layer) 1250×430×		
Paper	(double layer)	
Bamboo strips	900×2×2 900×3×3 900×6×1	

Table 2: Bamboo reference mechanical index.

Density 0.8g/cm3 Compressive strength	30MPa
---------------------------------------	-------

Current Research and Innovations Journal

Research Article

Parallel	grain	tensile	60MPa	Modulus of elasticity	6GPa
strength			oown a	Wiodulus of elasticity	oor a

3. Structure Selection

The choice of structural form of power tower should be based on the actual project span size, support conditions, plane style and other factors to implement the overall analysis to determine. Combined with the study and work experience, this experiment chose the lattice structure form.

3.1. Component Analysis

Compared with the performance of bamboo veneer, bamboo strips have a better uniformity and the ultimate load increases with the increase of specimen size. Bamboo strips have defect zones (nodes), and when the length of the specimen is lengthened, the size of the material is also increasing, and the chance of the material defect zones appearing at this time is also increasing [3]. Therefore, when the length of the structural specimen is longer, its ultimate load value will be lower.

The model formed moments during the stage of applying tensile load, which weakened the ability of the model to bear the load due to the relatively large torque effect on the overall structure, meanwhile, the modulus of elasticity of the bamboo strip was relatively large and ductile, which caused the eccentric moments to have a more significant effect on the ultimate bearing capacity of the bamboo strip [4]. The test results show that the smaller the specimen size is, the more significant the effect of eccentric moment on the ultimate bearing capacity is, and the larger the specimen size is, the weaker the effect of eccentric moment on the ultimate bearing capacity is, but the specimen is too long, which will affect the stability of the compression bar, so the specimen length in the final confirmation scheme is chosen moderate [5].

3.2. Column Design

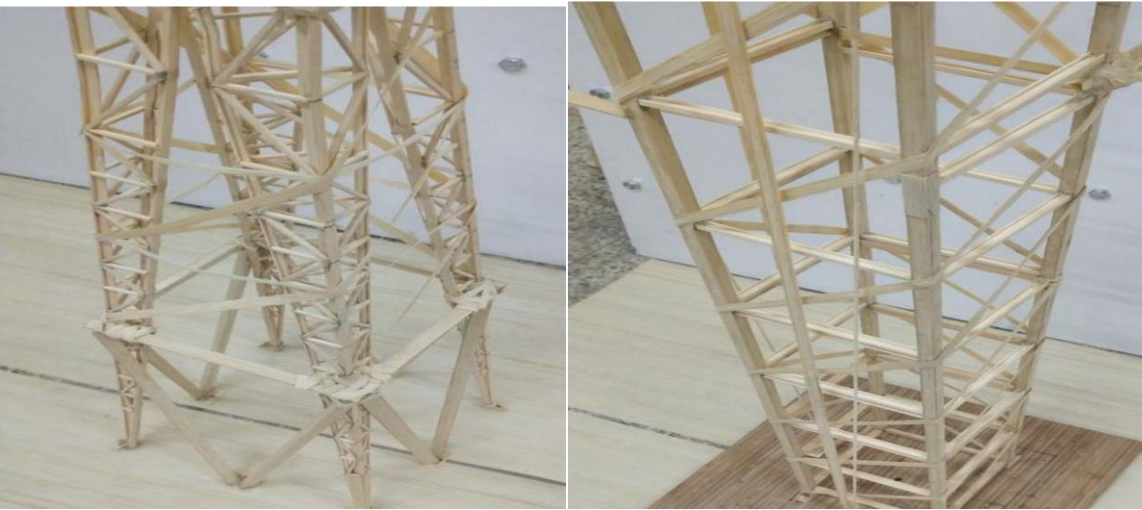
The columns mainly bear the combined effects of vertical load, torque and tension. Considering the stability of the triangular truss structure, a total of two column structures are designed on this basis.

In Fig. 2, a) the structural form of column is a space truss structure, using bamboo strips pasted into T-beam splicing, the process is simple and easy to make, the column is wide at the top and thin at the bottom, and the bottom is enlarged feet to enhance its stability, but the loading test found that the program is not enough torsional stiffness, deformation is larger, and the self-weight is larger [6]. b) The structural form of column II uses bamboo veneer to make hollow square column, with stiffening ribs at the node position. Ribs, four columns with the same spacing, between the column and the column using the tension bar to resist the torque, the test found that the method of lighter self-weight, and torsional stiffness is larger, can be good resistance to the level 2 load, once after a comparison, the final

<u>Current Research and Innovations</u> <u>Journal</u>

Research Article

determination of the column structure form using the b) Figure design [7].



a) Column structure form one Figure 2: Model of column structure.

b) Column structure form II

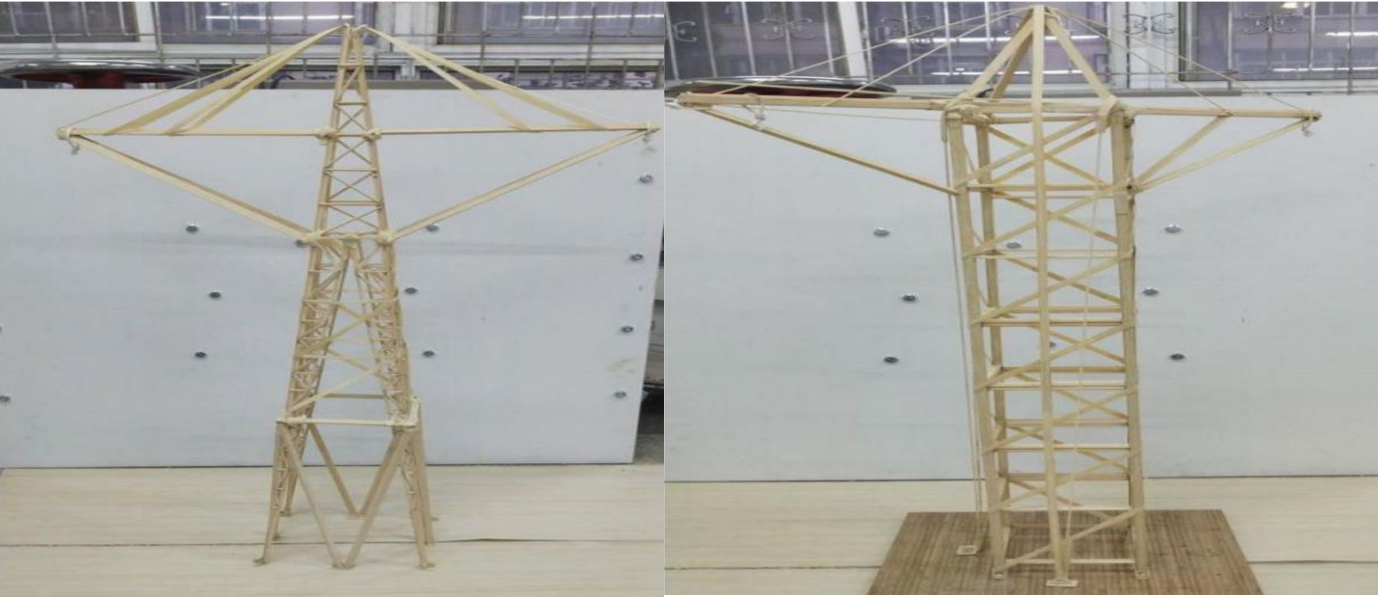
3.3. Main Structure Design

As shown in Figure 2 a), the main body of the model is designed and made into a truss system by bamboo strips in Scheme 1, and the oblique support system is added on the surface of each side of the truss structure, so that each surface is divided into individual small triangular structures, thus strengthening its structural stability [8]. The overall truss structure diagonal rods can all convey shear force well, while the deformation is small and the strength of the material can be utilized to the maximum [9]. The spatial layout of the model of Scheme 1 is symmetrical, flexible and rigid, but the torsional stiffness of the structure is insufficient, and the structure suffers torsional damage at $10 \text{cm}_30 \text{cm}$ below the low hanging point under Class 2 load, leading to structural failure [10].

As shown in Fig. 2 b), Scheme 2 designed the main body of the model in the form of lattice structure, and the four limbs of the structure were made of bamboo veneer paper to form a hollow square column section, and the four limbs relied on the tie bar to form a whole, which could play the role of torsional resistance, and the test proved that the tie bar had a good effect of torsional resistance [11]. The low hanging point bar can change the angle with the change of working condition to achieve effective bearing of three levels of load. It is verified by test that the scheme can better cope with various working conditions [12].

<u>Current Research and Innovations</u> **Journal**

Research Article



a) Option 1
Figure 3: Model processing diagram.

b) Option 2

4. Modeling

4.1. Component Material Analysis and Section Selection

According to the knowledge of civil engineering materials we know very well along the wood along the wood grain direction its tensile and compressive strength is greater, along the horizontal grain direction is the smallest[13]. see Figure 4, relative to the shear strength of the smallest shear strength direction is along the grain direction, in contrast to this along the horizontal grain direction is the largest, if the use of staggered grain adjacent veneer, although it can make the strength of each direction are very average, but the quality may not reach So the panel uses a single layer of vertical grain bamboo veneer paper, with bamboo veneer pulling strips at certain intervals horizontally, so that the vertical and horizontal strength of the panel does not differ much[14]. Therefore, it should be cut along the direction of the grain as much as possible when making the model.

| ISSN: 3065-0712 Page | 5

<u>Current Research and Innovations</u> **Journal**

Research Article

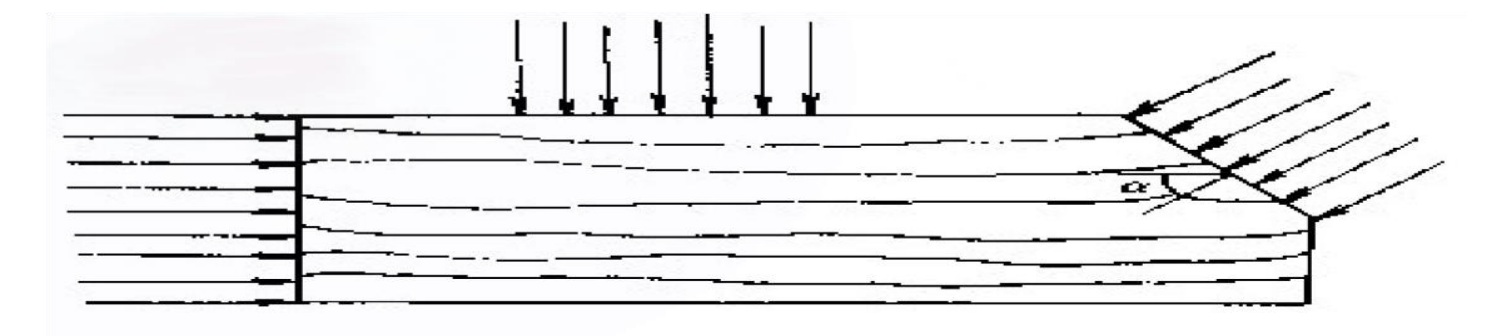
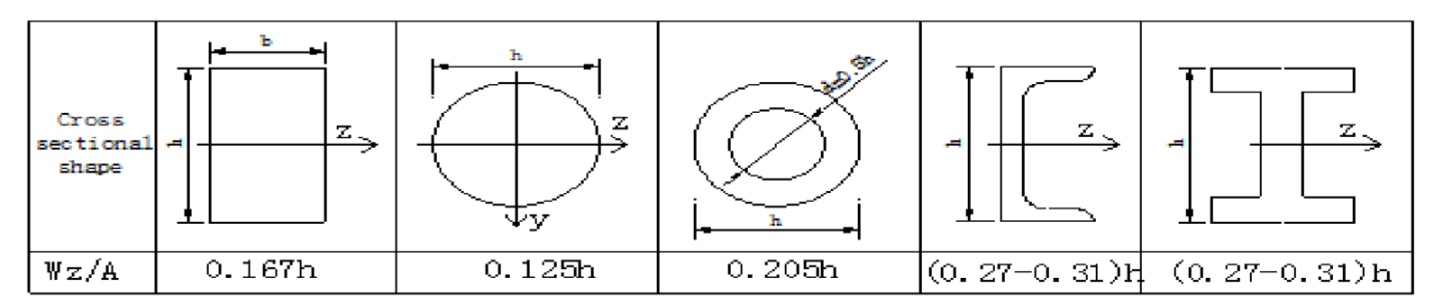


Figure 4: Bamboo veneer pattern.

According to the knowledge of material mechanics, the ideal cross-sectional style of the beam should be maximized without increasing the cross-sectional size. W_Z/A Such a cross-section is both suitable and economical [15]. The ratios of several common types of cross-sections W_Z/A are listed in Table 3. Table 3 shows that I-beam and slotted sections are more economical than rectangular sections, while rectangular sections are more economical than circular sections [16].

Table 3: WWzz/AA Values.



Therefore, when designing the cross-section of the beams in the model, rectangular cross-sections are used for the four main columns that mainly bear the combined effects of vertical load, torque and tension, and the shear effects are ignored for the other support system members of the structure, and I-beam cross-sections are partially selected under the consideration of the effects of bending moments, and T-shaped cross-sections.

4.2. Node Construction

Since the connection between the members of the model is made by glue bonding, in order to make the connection between the members more secure and the model structure lighter in weight and more stable, the nodes should have a large contact surface with each other and reduce the material consumption at the same time [17]. Therefore, after several experiments we model node connection using two forms of Figure 5. According to the basic knowledge of mechanics, so in the subsequent modeling, the nodes between members are connected by rigid joints.

<u>Current Research and Innovations</u> <u>Journal</u>

Research Article

5. Loading and Finite Element Analysis





a) Node construction I Figure 5: Node construction diagram

b) Node construction II

5.1. Loading Overview

The loading facilities of the model are mainly composed of the downhill gantry, the bearing plate, the uphill gantry and the lateral loading frame, as shown in Figure 6. The downhill and uphill gantry have 2 "low hanging points" and 1 "high hanging point" respectively, and the wires are manually hung on the corresponding hanging points of the downhill gantry, the model and the uphill gantry before loading as required. The wires are hung on the corresponding hanging points of the downhill gantry, model and uphill gantry manually before loading, as shown in Figure 6.

The position of the uphill gantry is unchanged during the experiment, and the downhill gantry can be rotated horizontally around the o point, and the rotation angle is 0° , 15° , 30° and 45° for selection (Figure 6 takes the rotation of 30° as an example).

Before the experiment, the base plate was fixed on the bearing plate, and the wires, loading discs and horizontal wires were hung on the model according to the loading conditions extracted, which was called the "no-load" stage, while three laser distance meters were placed on the bearing plate at the bottom of the loading disc in the middle of each wire to measure the distance from the bottom of the loading disc to the face of the bearing plate. The distance between the bottom of the loading plate and the surface of the bearing plate.

| ISSN: 3065-0712 Page | 7

<u>Current Research and Innovations</u> <u>Journal</u>

Research Article

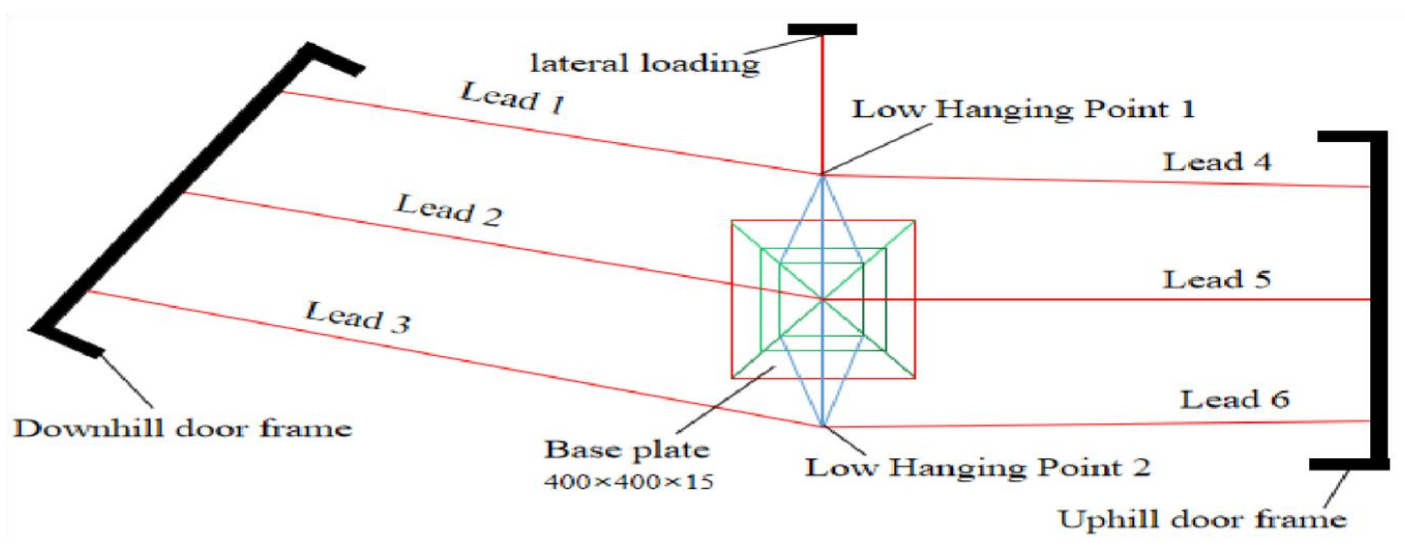


Figure 6: Schematic of wire suspension.

In the loading process, according to the provisions of Table 4, it is necessary to ensure that the clearance height from the bottom surface of the loading plate to the surface of the bearing plate in the middle part of each conductor shall not be less than its corresponding value, otherwise it will be judged that the geometry of the model does not match or the level of loading fails.

Table 4: Clearance limits between the bottom surface of the loading plate and the surface of the bearing plate.

Wire number	1	2	3	4	5	6
Clearance limit (mm)	400	600	400	800	1000	800

And according to the experimental requirements, the wire loading conditions have the following four for selection, as shown in Table 5.

Table 5: Lead wire loading conditions.

Number Work conditions	Lead 1	Lead 2	Lead 3	Lead 4	Lead 5	Lead r 6
A	$\sqrt{}$	$\sqrt{}$				V
В	$\sqrt{}$				V	V
С		$\sqrt{}$	$\sqrt{}$	V		
D			V		$\sqrt{}$	

5.1.1. Overview of Loading at All Levels

| ISSN: 3065-0712 | Page | 8

<u>Current Research and Innovations</u> **Journal**

Research Article

One-stage loading: (1) Pick one of the 3 loading wires and give weights on the loading disc of its picked wire, then the total weight of the applied weights at this stage is counted as M1, as shown in Fig. 7 a) (with the working condition A rotated by 30° for example, the same below). (2) When the loading is finished, it needs to stay for 10s, and then it needs to obtain the headroom height information of the 3 laser rangefinders under the loading disc, if the headroom height information is less than the requirement of Table 4 or the display is abnormal, the loading will be regarded as a failure.

Secondary loading: (1) The first-level load applied in the previous part will be held, while weights are applied on the loading disc for the remaining 2 specified wires, then the total weight of the applied weights at this level is counted as M2, as shown in Figure 7b). (2) When the loading is finished, it needs to stay for 10s, and then the headroom values of the 3 laser distance meters under the loading disc need to be obtained, and if the values are less than the requirements of Table 4 or show abnormalities, the loading will be judged to have failed.

Three levels of loading: (1) the first and second levels of loading applied in the previous part remain unchanged. At the same time, the lateral horizontal load is given at the location of the "horizontal loading point" of the model using the "weight + guide rope" requirement, and the size of the applied load weight can be chosen between 4kg and 10kg, which is M3, as shown in Figure 7c). (2) When the loading is finished, it is necessary to stay for 10s, after which if the model overturns or collapses as a

whole, or if the wire falls or is unhooked, the loading will be judged to have failed.

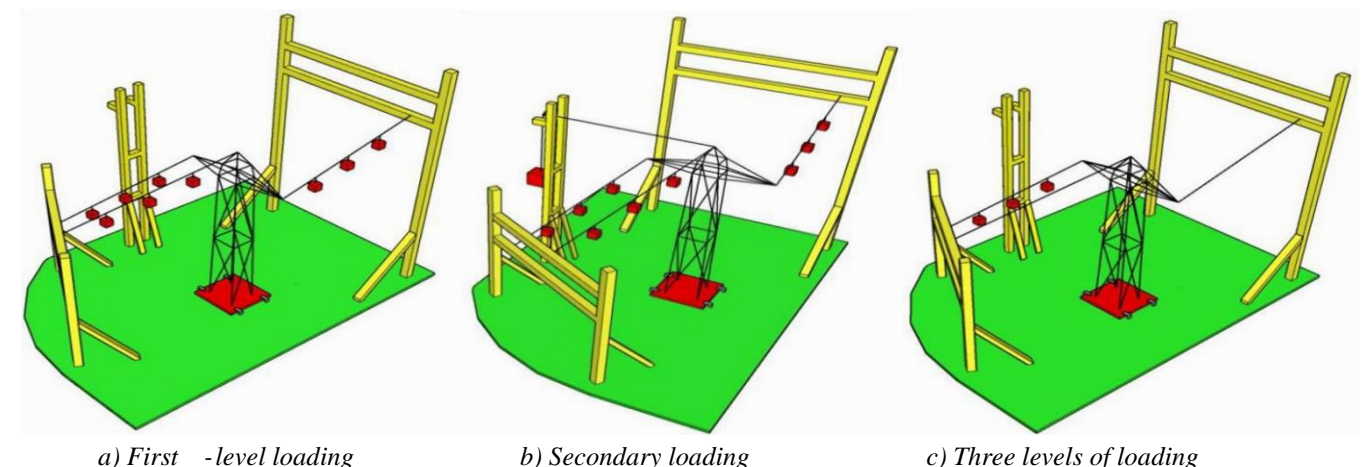


Figure 7: Loading schematic.

5.2. Finite Element Analysis

According to the experimental requirements, the four loading conditions and the rotation angles of 0°, 15°, 30° and 45° were loaded respectively in Table 5. According to the structural model, the structure was simulated by the finite element ANSYS software, and the rods were simulated by the built-in BEAM188 unit of ANSYS software, and the material parameters were taken according to Table 2[6]. Through the static analysis, the finite

| ISSN: 3065-0712 Page | 9

<u>Current Research and Innovations</u> <u>Journal</u>

Research Article

element model and the structure equivalent force cloud and Z to displacement cloud two results were extracted, respectively, from the strength and stiffness of the structure in the loading process of the two aspects of the force under all levels of load. The tensile strength of bamboo is 30 MPa, and the structure may be damaged once the equivalent force exceeds the theoretical ultimate tensile stress.

5.2.1. Finite Element Model

According to the above model appearance size requirements, loading requirements, we take the actual model for example; Figure 8 shows the complete finite element model.

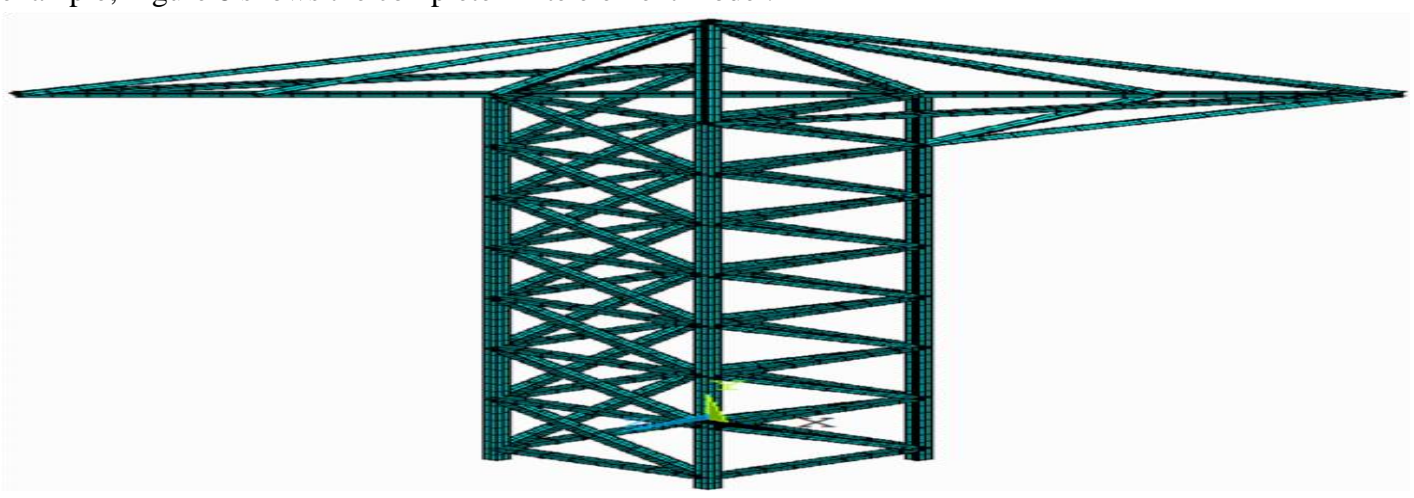
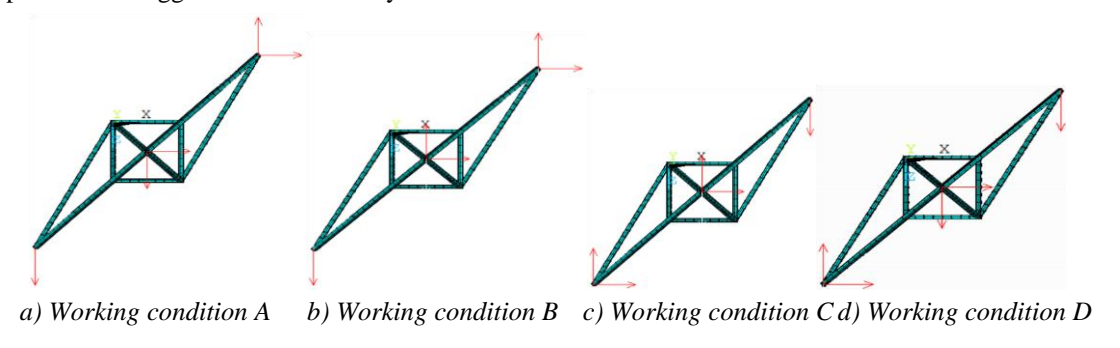


Figure 8: Finite element model.

5.2.2. Analysis of Working Conditions

According to the experimental requirements of, the four loading conditions and rotation angles of 0° ,

15°, 30° and 45° were used in Table 4-2, and the loads were loaded in accordance with the full load of 4kg in the first level, 3kg in the second level and 10kg in the third level. For simplicity, this section only shows the finite element analysis of the four loading conditions with the rotation angle of 30°, and outputs the displacement cloud in Z direction and the equivalent force cloud, and gives the model optimization suggestions for the analysis results.



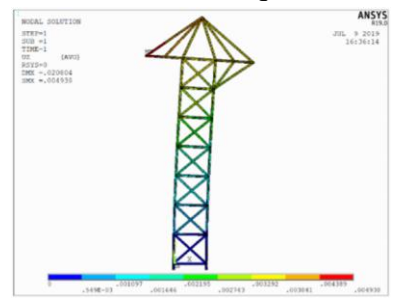
| ISSN: 3065-0712

<u>Current Research and Innovations</u> **Journal**

Research Article

Figure 9: Loading diagram with a rotation angle of 30°.

Condition A: The loading method is 4kg for primary load, 3kg for secondary load, and 10kg for tertiary load, and the results of ANSYS simulation are shown in Figure 10 and Figure 11. According to the calculation, the maximum equivalent force of the overall structure is 54.7MPa, and the tensile strength of bamboo veneer paper is 60MPa, which meets the requirements, the maximum equivalent force is located at the foot of the column, so the foot of the column needs to be focused on. According to the test measurement, the sinkable limit is 115mm. According to the finite element calculation result, the Z-directional displacement deformation value is 4.9mm, which meets the requirement.



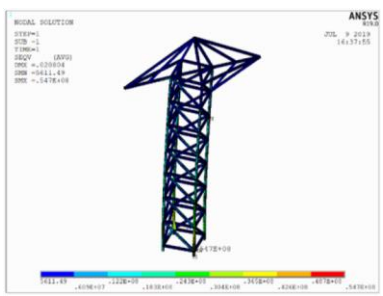


Figure: 10 Z-direction displacement cloud. Figure 11: Equivalent force cloud.

Condition B: The loading method is 4kg for primary load, 3kg for secondary load, and 10kg for tertiary load, and the results of ANSYS simulation are shown in Figure 12 and Figure 13. According to the calculation, the maximum equivalent force of the overall structure is 52.6MPa, and the tensile strength of bamboo veneer paper is 60MPa, which meets the requirements, the maximum equivalent force is located at the foot of the column, so the foot of the column needs to be focused on. According to the test measurement, the sinkable limit is 115mm. According to the finite element calculation result,

the Z-directional displacement deformation value is 12.4mm, which meets the requirement.

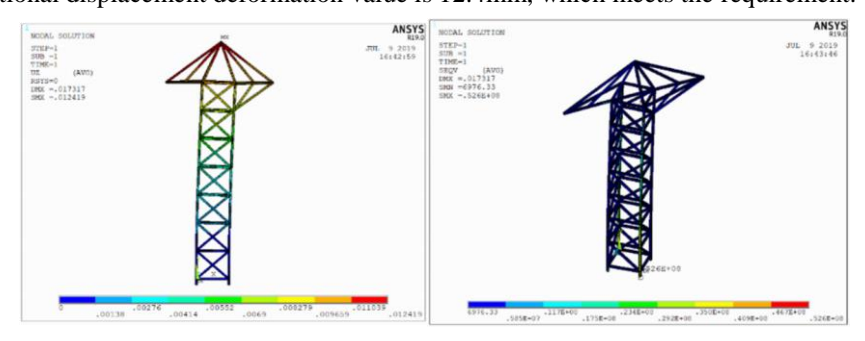


Figure 12: Z-direction displacement cloud. Figure 13: Equivalent force cloud.

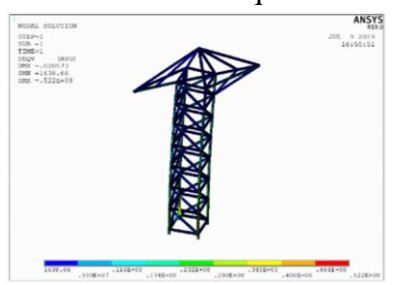
(3) Condition C: The loading method is 4kg for primary load, 3kg for secondary load, and 10kg for tertiary load, and the results of ANSYS simulation are shown in Figure 14 and Figure 15. According to the calculation,

| ISSN: 3065-0712 Page | 11

<u>Current Research and Innovations</u> **Journal**

Research Article

the maximum equivalent force of the overall structure is 52.2MPa, and the tensile strength of bamboo veneer paper is 60MPa, which meets the requirements, the maximum equivalent force is located at the foot of the column, so the foot of the column needs to be focused on. According to the test measurement, the sinkable limit is 115mm. According to the finite element calculation result, the Z-directional displacement deformation value is 3.9mm, which meets the requirement.



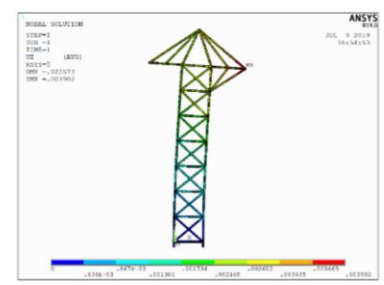
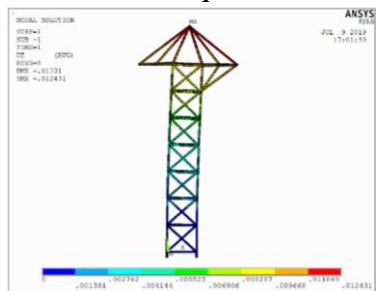


Figure 14: Z-direction displacement cloud. Figure 15: Equivalent force cloud.

Condition D: The loading method is 4kg for primary load, 3kg for secondary load, and 10kg for tertiary load, and the results of ANSYS simulation are shown in Figure 16 and Figure 17. According to the calculation, the maximum equivalent force of the overall structure is 52.7MPa, and the tensile strength of bamboo veneer paper is 60MPa, which meets the requirements, the maximum equivalent force is located at the foot of the column, so the foot of the column needs to be focused on. According to the test measurement, the sinkable limit is 115mm. According to the finite element calculation result, the Z-directional displacement deformation value is 12.4mm, which meets the requirement.



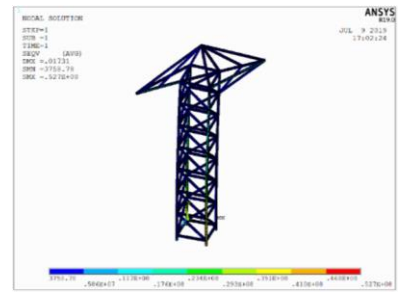


Figure 16: Z-direction displacement cloud. Figure 17: Equivalent force cloud.

Due to space reasons this section only shows the model to rotate the angle of 30° as an example of finite element analysis, other angles of the data analysis is shown in Table 6, from the table data can be seen that the model for the experimental various conditions of its equivalent pressure maximum and Z-directional displacement values are to meet the bamboo veneer paper smooth grain tensile strength of 60MPa, sinking displacement limit of 115mm, the model structure is reliable.

Table 6: Working condition analysis data sheet.

| ISSN: 3065-0712

Current Research and Innovations Journal

Research Article

Angle	Work	Equivalent pressu	re Z-directional displacement
conditions		maximum	value
	A	42.3MPa	6.25mm
0°	В	42.8MPa	13.5 mm
	С	42.4MPa	6.05mm
	D	42.8MPa	13.4mm
	A	23.1MPa	9.84mm
15°	В	43.5MPa	11.7mm
	С	48.5MPa	4.97mm
	D	33.4MPa	11.4mm
30°	A	54.7MPa	4.9mm
	В	52.6MPa	12.4mm
	С	52.2MPa	3.9mm
	D	52.7MPa	12.4mm
45°	A	41.2MPa	2.56mm
	В	34.6MPa	12.2mm
	С	37.9MPa	3.34mm
	D	44.3MPa	12.3mm

6. Summary

This paper carries out the structural selection, modeling and finite element analysis of the power tower model, the angle of rotation of the model, different working conditions for the graded loading analysis of the strength and stiffness of the internal structure of the power tower, to obtain the corresponding stress and Z-directional displacement shape of the structure, pointing out the equivalent force maximum parts, and compared with the experimental limits of each working condition, to meet the relevant provisions, the model structure is reliable.

References

Bezas M Z, Jaspart J P, Vayas I, et al. Design recommendations for the stability of transmission steel lattice towers. Engineering Structures, 2022, 252: 113603.

Huang Wenhu. Optimization analysis of bridge structure in structural design competition for college students. Shanxi Architecture, 2022, 48(08):76-80.

Xie Yufeng, Xu Ji, Xu Kaiao, Liang Chao-Feng, Shen Yiming. Model making process and assembly method of structural design competition for university students. Urban Architecture, 2021, 18(32):157-159.

| ISSN: 3065-0712 Page | 13

<u>Current Research and Innovations</u> **Journal**

Research Article

- Song Xiaobing, Wu Xiaoang, Yan Bin, Meng Jingxi, Chen Sijia. Design principles and case studies of structural design competition schemes for university students. Mechanics and Practice, 2020, 42(03):388-393.
- Hosseini N, Ghasemi M R, Dizangian B. ANFIS-based optimum design of real power transmission towers with size, shape and panel design variables using BBO algorithm. IEEE Transactions on Power Delivery, 2021, 37(1): 29-39.
- Li Y, Yan Z, Zhou D, et al. Analysis of the stability behavior of cross bracings in transmission towers based on experiments and numerical simulations. Thin-Walled Structures, 2023, 185: 110554.
- Zhang G, Zhang H, Peng H, et al. Dynamical shakedown analysis of high-rise tower structure. Engineering Computations, 2021.
- Ma L, Khazaali M, Bocchini P. Component-based fragility analysis of transmission towers subjected to hurricane wind load. Engineering Structures, 2021, 242: 112586.
- Zhao S, Yan Z, Savory E. Design wind loads for transmission towers with cantilever cross-arms based on the inertial load method. Journal of Wind Engineering and Industrial Aerodynamics, 2020, 205: 104286.
- Shukla V K, Selvaraj M, Kumar K V. Failure Analysis of a Cruciform-Leg Transmission Line Tower. International Journal of Steel Structures, 2021, 21: 539-548.
- Gao X, Yi R, Zhang L, et al. Failure Analysis of Transmission Tower in Full-Scale Tests. Buildings, 2022, 12(4): 389.
- Xie Q, Zhang J. Experimental study on failure modes and retrofitting method of latticed transmission tower. Engineering Structures, 2021, 226: 111365.
- Roy S, Kundu C K. State of the art review of wind induced vibration and its control on transmission towers[C]//Structures. Elsevier, 2021, 29: 254-264.
- Fu X, Du W L, Li H N, et al. Stress state and failure path of a tension tower in a transmission line under multiple loading conditions. Thin-Walled Structures, 2020, 157: 107012.
- Fu Z, Tian L, Liu J. Seismic response and collapse analysis of a transmission tower-line system considering uncertainty factors. Journal of Constructional Steel Research, 2022, 189: 107094. [16] Fu X, Li H N, Li G, et al. Fragility analysis of a transmission tower under combined wind and rain loads. Journal of Wind Engineering and Industrial Aerodynamics, 2020, 199: 104098. [17] Zhang Y, Huang W, Wang L. Wind Field Characteristics of Butte and the Influence on the Wind-Induced Responses of Transmission Towers. Advances in Materials Science and Engineering, 2022, 2022.